

# The effect of collagen/polycaprolactone fibrous scaffold decorated with graphene nanoplatelet and low-frequency electromagnetic field on neuronal gene expression by stem cells

Marzie Moraveji<sup>1,2</sup>, Hamid Keshvari<sup>\*2</sup>, Akbar Karkhaneh<sup>2</sup>, Shahin Bonakdar<sup>1</sup>,  
Amin Hadi<sup>3</sup> and Nooshin Haghighipour<sup>\*\*1</sup>

<sup>1</sup>National Cell Bank of Iran, Pasteur Institute of Iran, Tehran, Iran

<sup>2</sup>Department of Biomedical Engineering, Amirkabir University of Technology, Tehran, Iran

<sup>3</sup>Cellular and Molecular Research Center, Yasuj University of Medical Sciences, Yasuj, Iran

(Received September 29, 2020, Revised March 14, 2021, Accepted March 16, 2021)

**Abstract.** This study aimed to develop a collagen/polycaprolactone (CP) fibrous scaffold decorated with Graphene (Gr) nanoplatelets (Gr-CP). In previous studies, accessibility of cells to the surface of Gr nanoplatelet was missed. Nanofibers were prepared by electrospinning which sprayed Gr nanoplatelets (1 wt.%) to synthesize the Gr-CP scaffold. Fourier transform infrared spectroscopy (FTIR) was utilized for investigation of chemical structure. Tensile tests were performed to study the influence of Gr on the mechanical properties of scaffolds. Cell differentiation was analyzed based on MAP2 and TUJ1 expression levels using real-time PCR technique in 6 groups. The variables examined in this experiment was the neural differentiating chemical medium, low-frequency electromagnetic field (LFEMF; 50Hz, 1mT) and Gr. Based on the results, Young's modulus, tensile strength and work of fracture ratio of the Gr-CP were 1.68, 2.41 and 1.42 times higher than those of the CP scaffold, respectively. MTT assay outcomes were indicative of scaffold cytocompatibility. The group treated with all three factors exhibited the highest MAP2 expression level compared to other groups. Based on the obtained results, exposing stem cells to the combined treatment of Gr and LFEMF can be used as a promising method to induce neuronal differentiation.

**Keywords:** low-frequency electromagnetic field; graphene; nanofiber; neuron, cell differentiation; gene expression

## 1. Introduction

Spinal cord injuries can cause damages to neurons, oligodendrocytes and lead to axon demyelination. There are three strategies to regenerate an injured nerve, including tissue engineering, molecular and biomaterial based approaches. As a branch of regenerative medicine, tissue engineering involves the utilization of cells (mature or stem cells), signaling factors (such as chemical, magnetic, electrical and mechanical signals) and scaffold as a microenvironment for cell attachment, differentiation and migration (Lanza *et al.* 2013, Rastin *et al.* 2020, Rastin *et al.* 2020, Rohani Rad *et al.* 2019).

In addition to chemical stimuli as the most widely used signaling factors for cell differentiation, electrical, magnetic and low-frequency electromagnetic fields (EMF) have been recently assessed for application as signaling factors, as well. EMF has been generally reported to affect cell behavior, especially differentiation. EMF with different frequencies has induced cell differentiation toward neural (Barati *et al.* 2020, Barati *et al.* 2020b, Khoram *et al.* 2020,

Lee *et al.* 2015, Moraveji *et al.* 2016, Najafzadeh *et al.* 2020), chondrogenic (Kavand *et al.* 2016), osteogenic (Jazayeri *et al.* 2016, Ongaro *et al.* 2014), cardiac muscle (Gaetani *et al.* 2009) and skeletal muscle (Norizadeh-Abbariki *et al.* 2014) cells. One of the main mechanisms of EMF effect on cells involves ion channels and ion flow into and out of cells (Levin 2009). In this research, the effect of low-frequency electromagnetic field (LFEMF), as a potential signaling factor for cell differentiation, has been studied. The electromagnetic field can modulate the hyperpolarizing potassium channels by increasing the intracellular calcium concentration (Tonini *et al.* 2001). However, some reports suggest that the electromagnetic or magnetic fields have no effect on this phenomenon (Madec *et al.* 2003). Magnetic and electromagnetic fields can affect the formation and rotation of protein molecules (Binhi *et al.* 2001, Laurence *et al.* 2000). Cheng and Zou (2006) showed that the electromagnetic field could separation of nucleotide sequences and unwinding of a double helix during DNA replication. Buchachenko *et al.* (2007) indicate that the electromagnetic field increase the production of ATP molecules in the cell. The magnetic field increases phosphorylation up to 2 times and also affects the calcium bind (Markov and Pilla 1997). Wang *et al.* (2009) showed that the average magnetic field interferes with cellular signals, some membrane lipids, calcium flow, and the expression of some genes. Extremely low-frequency

\*Corresponding author, Associate Professor,

E-mail: [haghighipour@pasteur.ac.ir](mailto:haghighipour@pasteur.ac.ir)

\*\*Co-corresponding author, Assistant Professor,

E-mail: [keshvari@aut.ac.ir](mailto:keshvari@aut.ac.ir)

electromagnetic fields promote in vitro neuronal differentiation and neurite outgrowth of embryonic neural stem cells via up-regulating TRPC1 (Ma *et al.* 2016). Özgün *et al.* (2019) indicated that low-frequency magnetic fields can activate N-methyl-D-aspartate receptors in glutamatergic  $\text{Ca}^{2+}$  channels to promote neuronal differentiation.

As a microenvironment for cells, the scaffold can affect intracellular signals and control cellular behavior and activities. Biomimetic scaffolds that simulate extracellular matrix (ECM) are appropriate microenvironments for cells. Biopolymer nanofibers are among ECM components (Szymanski *et al.* 2014). Inspired by ECM structure, nanofibrous scaffolds have been synthesized for tissue engineering, using various techniques such as electrospinning (Teo and Ramakrishna 2006), self-assembly (He *et al.* 2014), phase separation (Vasita and Katti 2006) and template directed approaches (Acar *et al.* 2011) among which, electrospinning is a low cost and feasible method, compared to others (Golafshan *et al.* 2017). As neural cells tend to align on nanofibers and elongate along them, nanofibrous scaffolds have been extensively used in neural tissue engineering (Xie *et al.* 2009).

Various natural and synthetic polymers have been utilized to produce scaffolds for neural regeneration. Natural polymers show biological activity and synthetic polymers are associated with superior mechanical properties compared to the natural ones. Therefore combining natural and synthetic polymers can result in improved properties. As a natural polymer, collagen is well able to control cell behavior. In addition to its differential role, collagen causes the synapsis maturation of neurons and their release through the MAPK/ERK1/2- synapsin I intracellular signaling pathway (Yin *et al.* 2014). Synthetic polymers such as PGA (Yoshitani *et al.* 2007), PCL (Çapkın *et al.* 2012, Schnell *et al.* 2007), PLGA (Ouyang *et al.* 2013), PMMA (Li *et al.* 2008) can be combined with collagen to produce a neural tissue engineering scaffold. In particular, PCL fibers have the potential of inducing neural differentiation. For example, cells cultured on a PCL fibrous scaffold have been reported to express mature neuron markers such as MAP2 and  $\beta$ -tubulin, compared to control cells (Xie *et al.* 2009).

Depending on the type of tissue, specific characteristics are required for an appropriate tissue engineering scaffold. Conductivity is among the necessary properties of neural scaffolds. There are two types of synapses through which neighboring neurons communicate with each other: chemical synapses by a neurotransmitter and electrical synapses (Pereda 2014). A conductive scaffold seems to be capable of improving electrical synaptic transmission between neurons. In this regard, conductive biomaterials such as graphene (Gr) (Gupta *et al.* 2019, Soleimani *et al.* 2019, Zhang *et al.* 2018), carbon nanotube (CNT) (Xia *et al.* 2019), polyaniline (Garrudo *et al.* 2019), polypyrrole (Alegret *et al.* 2018), poly (3,4- ethylenedioxythiophene): poly (styrenesulfonate; pedot: pss) (Magaz *et al.* 2020) and MXene (Driscoll *et al.* 2018, Wychowanec *et al.* 2020), have been recently considered for application in neural scaffolds.

As a carbon derivative, Gr is a flexible, conductive, high strength, hard and biocompatible biomaterial (Ryu and Kim 2013). It can adsorb small biomolecules on its surface and thereby act as an appropriate substrate for cell activities (Park *et al.* 2011).

Park *et al.* (2011) have reported that Gr induces stem cells toward neuronal cells (by increasing TUJ1 expression) compared to astrocyte parenchymal cells (with decreased GFAP levels). In addition to cell differentiation, cell-cell communication and synaptic activity are also essential for the nervous system. Gr stimulates the neurite growth from the cellular body of neural cells (Li *et al.* 2011). Indeed, Gr causes the formation of neural network between the neural cells (Kenry *et al.* 2018). One of the obstacles in nerve regeneration is the secretion of inflammatory factors by glia cells. 2D and 3D Gr scaffolds can decrease inflammatory secretion and improve neurosphere formation and cell migration (Li *et al.* 2011).

A scaffold with structure of fiber/Gr is taken into consideration recently. 3D- printed PCL/rGO scaffold with conductive fiber structure has been introduced as an appropriate substrate for neural cell differentiation with expression of neural genes (TUJ1, NF-H, and GAP43) (Vijayavenkataraman *et al.* 2018). Also, it was shown that Gr can improve the differentiation of stem cell to dopaminergic neurons (Ginestra 2019). Although conducting the fiber with Gr is an exciting method, however the percentage of Gr effect on the properties of scaffold. For example, high percentage of Gr increases the hydrophobicity of scaffold and decreases the cell attachment and spreading on it (Golafshan *et al.* 2017). Coating of nanofiber with single sheet graphene is another technique for conduction of nanofiber with Gr. This method cannot disorder the alignment of nanofiber. GO coating increases the neurite-bearing PC12 cells and length of them. In fact, GO can stimulate cell differentiation for neural tissue engineering (Zhang *et al.* 2016).

Considering Gr conductivity, the combined treatment of Gr and electrical signals have recently attracted scientific attention. In this work, we used electrospinning to prepare PCL/collagen nanofibrous scaffolds which were modified with Gr nanoplatelet spraying during synthesis. The difference of this work with other studies based on electrospinning and Gr is that the Gr nanoplatelet was not distributed in electrospinning solution. As a result, Gr nanoplatelet placed on the fibers instead of embedded inside of them. It is noteworthy that the cells miss the direct contact with Gr when they are inside of fibers. We investigated the effect of Gr on the mechanical properties of the scaffold. Another aim of this research was to assess the effect of Gr on adipose mesenchymal stem cells (AMSCs) differentiation based on the expression of neuronal markers. In addition, the effect of LFEMF was also investigated using real-time PCR. The simultaneous effects of Gr and LFEMF on AMSCs differentiation were studied.

## 2. Materials and methods

### 2.1 Fabrication of Gr-CP fibrous scaffold

Gr-CP fibrous scaffold was prepared using two techniques, namely electrospinning and spraying. It was necessary first to prepare polymeric and Gr solutions. The polymeric solution was prepared from 15 wt.% collagen I (National cell bank of Iran) and PCL (Mn = 80,000, sigma Aldrich) within 90% acetic acid solvent, with a collagen/PCL ratio of 25/75 wt.%. To prepare PCL solution, PCL pellet in 90% acetic acid was placed on a hot plate stirrer at 50°C for 90 min. To prevent collagen denaturation at high temperatures, collagen was added to the solution after the PCL solution cooled down. After 40 min, the CP solution was ready to use. To obtain Gr-CP fibrous scaffold with 1 wt.% Gr, Gr nanoplatelets (purity > 99.5%; less than 32 Layers, Nanosany Corporation, Iran) were dispersed in DMF using a probe sonicator (100 W) for 90 min. For the electrospinning process, CP solution was fed into 1 mL insulin syringes. Electrospinning parameters including voltage, flow rate, tip to collector distance and rotational speed of collector were set to 22 kV, 0.3 mL/h, 13 cm and 700 rpm, respectively. Every half hour, at zero flow rate and zero voltage, the dispersed graphene was sprayed on the nanofibers. The appropriate distance of sprayer and collector caused the sprayed droplets to spread on the fibrous scaffold uniformly. After scaffold fabrication, cross linking was performed using 10% or 25% glutaraldehyde (GA) vapors at room temperature for 72 or 24 h, respectively. For complete solvent evaporation after scaffold cross linking, the scaffold was placed in a vacuum oven at 25°C for 24 h.

### 2.2 Characterization of Gr-CP fibrous scaffold

Nanofiber morphology, as well as distribution and dispersion of graphene nanoplatelets on the surface of nanofibers were studied via scanning electron microscopy (SEM, AIS 2100, Seron Technology, Korea). Nanofiber diameter (n = 25) was determined using Image J software 1.44 p.

Chemical composition of scaffold and the effect of cross linking were studied through Fourier transform infrared spectroscopy (FTIR) over the range of 400-4000 cm<sup>-1</sup>.

Mechanical properties were investigated using a tensile testing machine (GALDABINI, Italy). Two 20 mm × 5 mm specimens of Gr-CP and CP nanofibrous scaffolds with 10 μm and 30 μm thickness values, respectively, were tested using an extension rate of 1.0 mm/min. The obtained data were used to calculate Young's modulus, tensile strength and toughness of specimens.

### 2.3 Cell study

#### 2.3.1 Extraction test and cell proliferation study

To investigate the effects of scaffold on cell proliferation, extract test was performed according to ISO 10993-5 guidelines. In this test, 1 ml of culture media (DMEM containing 10% (v/v) FBS) per 6 cm<sup>2</sup> of the

scaffold was added to a 6-well plate and incubated at 37°C and 5% CO<sub>2</sub> for 24 h. Before performing the extract test, each side of scaffold was sterilized under UV light for 45 min and washed thrice with sterile PBS. It should be noted that sterilizing collagen with UV for less than an hour has no effect on collagen (Sionkowska *et al.* 2020). Concurrent with the start of the extraction test, 10<sup>4</sup>, L929 cells were seeded on a 96-well plate. After 24 h, the culture medium of L929 cells was replaced with 100 μl of scaffold extract. The control sample was incubated with DMEM containing 10% (v/v) FBS. Cell proliferation was studied based on 3-(4,5-dimethylthiazolyl-2)-2,5-diphenyl tetrazolium bromide (MTT) assay. After 24 or 72 h, the culture medium was discarded, sample was rinsed with 1x PBS and cells (n = 5 for each group) were incubated with 100 μl of MTT solution (0.5 mg/ml MTT reagent in PBS) for 4 h. Finally, MTT solution was removed, and violet formazan crystals were dissolved in 100 μl of isopropanol for 20 min. The optical density (OD) of formazan was measured using an Eliza reader machine (Stat Fax 2100, Awareness Technology, US) at 545 and 630 nm wavelengths. The relative cell proliferation was calculated based on Eq. (1) (Mohabatpour *et al.* 2016)

$$\text{Relative cell proliferation} = \frac{\text{mean OD of sample}}{\text{mean OD of control}} \times 100 \quad (1)$$

#### 2.3.2 SEM analysis of cell attachment and cell morphology on the Gr-CP scaffold

To image the cells cultured on the scaffold, 50×10<sup>4</sup> L929 cells were first seeded on the scaffold for 24 h. After fixing the cells with GA 4% (v/v) for 4 h at 4°C, the scaffold was rinsed with PBS and dehydrated using a graded ethanol series (30, 50, 70 and 95%). After drying the scaffold and coating with gold, SEM analysis was carried out.

#### 2.3.3 Cell differentiation

Rat adipose mesenchymal stem cells (RAMSCs) were obtained from National Cell Bank of Iran and cultured in a media consisting of DMEM/F12 + 10% (v/v) FBS + 1% (v/v) penicillin/ streptomycin. Scaffold sterilization was the prerequisite of study. In this investigation, six groups were studied during 13 days, in which passage 3 cells were cultured on: 1) Gr-CP nanofibrous scaffold and subjected to LFEMF (Gr-CP(EM)), 2) Gr-CP nanofibrous scaffold and incubated with neural differentiation medium while being exposed to LFEMF (Gr-CP(ch-EM)), 3) CP nanofibrous scaffold and exposed to LFEMF (CP(EM)), 4) tissue culture polystyrene (TCPS) and subjected to LFEMF (TCPS(EM)) 5) Gr-CP nanofibrous scaffold and incubated with neural differentiation medium (Gr-CP(ch)), 6) TCPS. Neural differentiation medium contained DMEM/F12, 10%(v/v) FBS, 10 ng/ml b-FGF (Royan Institute,Iran), 10 ng/ml EGF (Gibco,UK), 5 mM retinoic acid (Sigma aldrich, USA) and 100 μM BHA (Sigma aldrich, USA).

LFEMF device, which had been previously designed and fabricated in National Cell Bank of Iran and could be placed in an incubator, consisted of a multi-turn solenoid, an electrical current source and an operative for generation of nonsinusoidal, pulsed electromagnetic fields. The

frequency and flux density of the applied EMF were 50 Hz and 1 mT, respectively, with a pulse period of 40 ms and duty cycle (on/ off) of 25/15. EMF was applied on cells for 13 consecutive days (7 h/day) (Cho *et al.* 2012, Moraveji *et al.* 2016, Piacentini *et al.* 2008).

### 2.3.4 RNA isolation and reverse transcription polymerase chain reaction

RNA isolation was performed using RNeasy Plus mini kit (Qiagen, Germany) for the six experimental groups, followed by optical density measurement of RNA using a Nanodrop instrument (NanoDrop, USA) and cDNA synthesis using Takara kit. Neural differentiation of RAMSCs was assessed based on mRNA levels of MAP2 and TUJ1 as the target genes, while  $\beta$ -actin was used as the housekeeping gene. mRNA expression level was evaluated in triplicate utilizing SYBR® Green Master Mix and ABI Step One real time- PCR instrument (Applied Biosystems, USA). Primers were designed using Primer Blast (NCBI), as the following: MAP2: forward 5'-CAAACGTCATTACTTTACAAC TTGA-3' and reverse 5'-CAGCTGCCTCTGTGAGTGAG-3'; TUJ1: forward 5'-TGGATGT CGTGAGGAAAGAAT - 3' and reverse 5'-TCATCCGTGTTCTCCACTAGC-3'.

### 2.3.5 Statistical analysis

The results of this study were expressed as mean $\pm$ SD. Each test was repeated 3 times. The normality test was done by Shapiro-Wilk method. ANOVA and Scheffe's tests (SPSS) were performed to determine the significance of the difference between experimental groups. The value of  $p < 0.05$  was considered statistically significant.

## 3. Results and discussion

### 3.1 Fabrication and characterization of the Gr-CP fibrous scaffold

Providing surface availability of Gr and CP nanofibers was the main reason for choosing the mentioned fabrication method. The electrospun fibrous scaffold composed of PCL and collagen was associated with an average diameter of  $238 \pm 97$  nm. During electrospinning Gr nanoplatelets dispersed in DMF were sprayed on the scaffold (Fig. 1(a)). Since DMF is a solvent for PCL (Qin and Wu 2012), Gr spraying resulted in the surface dissolution of PCL nanofibers. Therefore, the Gr nanoplatelets sprayed on the nanofibers exhibited stronger interactions with them, compared to what is observed in common deposition technique. It is noteworthy that due to DMF spraying, the thickness of the Gr-CP scaffold was less than that of the CP scaffold. Scaffold SEM imaging (Fig. 1(b)) indicated a fibrous scaffold decorated with Gr nanoplatelets with thickness values of 2-18 nm and diameters of 40-80 nm (Fig. 1(a)).

After scaffold fabrication, cross linking with GA was performed, mainly to increase collagen stability in cell culture medium. 10% and 25% of GA vapors were used for

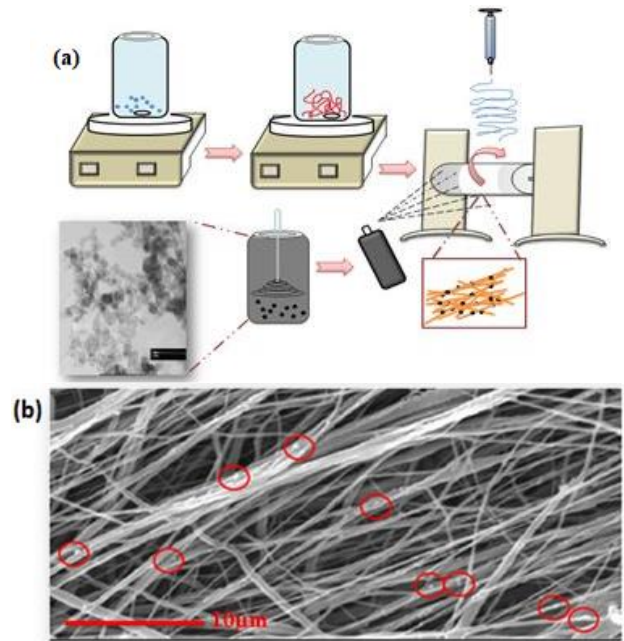


Fig. 1 Schematic diagram of Gr-CP scaffold fabrication and SEM image of it: a) preparation of nanofibers through electrospinning and decoration of the fibrous scaffold via Gr suspension spraying; b) SEM image of the fibrous scaffold decorated with Gr nanoplatelets. Red circles indicate Gr nanoplatelets on nanofibers.

cross linking to optimize the cytotoxicity and cross linking. Cross linking was analyzed through FTIR spectroscopy. The characteristic peaks of PCL in the cross linked and non-cross linked scaffolds were around 1175, 1240, 1294, 1418, 1729, 2867 and 2946  $cm^{-1}$ , attributed to the symmetric stretching COC, asymmetric stretching COC, stretching C-O, COO-, C = O, symmetric  $CH_2$  and asymmetric  $CH_2$  vibration, respectively (Rajzer *et al.* 2014) (as shown in Fig. 2(a)).

N-H peak was observed in the range of 3100-3400  $cm^{-1}$  (Li *et al.* 2003). As the frequency of band vibration is inversely proportional to the mass of vibrating molecule, the wavenumber peak of N-H was decreased in the cross linked scaffold. Reduction of  $NH_2$  and amide II formation was another consequence of cross linking (Damink *et al.* 1995). Therefore, the formation of amide II instead of  $NH_2$  caused an increase in the molecular weight, a decrease in vibration frequency and occurrence of red peak shifting (Fig. 2(a)). A higher Red peak shifting was observed in the 10% GA cross linked scaffold, compared to the 25% one.

Peaks observed at 1541 and 1652  $cm^{-1}$  for the cross linked scaffold were indicative of amide II and C = C bond (Coates 2000, Muyonga *et al.* 2004). Interaction of GA with collagen led to formation of amide II and decrease in  $NH_2$  (Fig. 2(b)). Interaction of two GA molecules resulted in C = C bond formation (Damink *et al.* 1995) (Fig.2 (b)). FTIR results were demonstrative of a greater reduction in primary amine groups in the scaffold cross linked with 10% GA, compared to that with 25% GA.

Mechanical properties such as Young' modulus, tensile strength and work of fracture are important factors of a

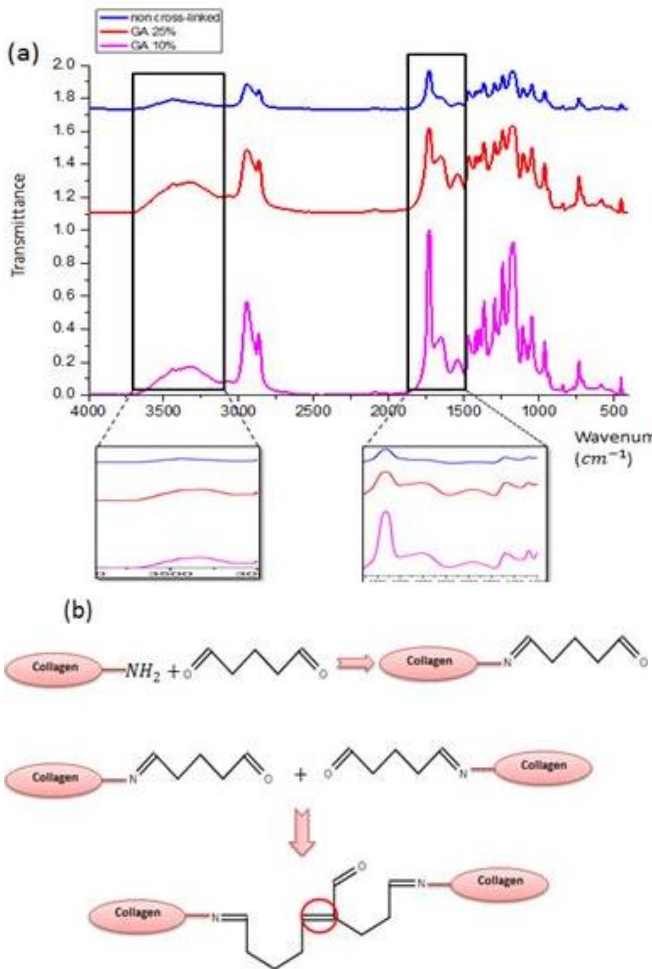


Fig. 2 Mechanism of crosslinking and FTIR analysis of it. a) FTIR spectra of non-cross linked and cross linked fibrous scaffolds with 10% and 25% GA; b) mechanism of collagen cross linking with GA

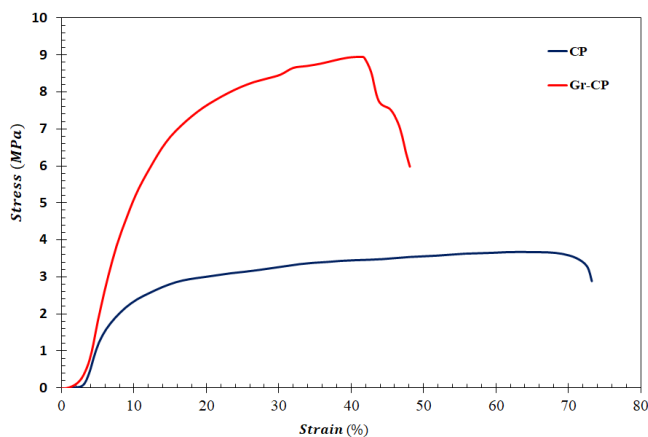


Fig. 3 The mechanical properties of CP and Gr-CP scaffolds. Young modulus, work of fracture and tensile strength of the Gr-CP scaffold were all greater than those of the CP scaffold.

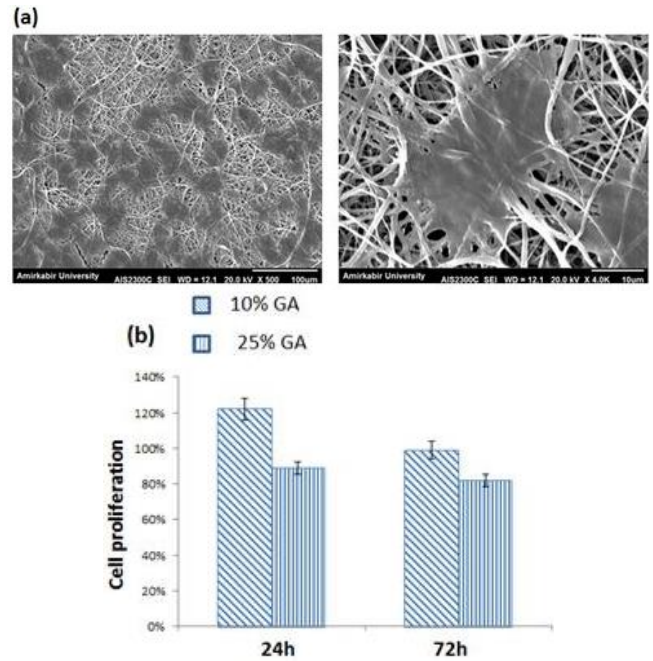


Fig. 4 Biocompatibility analysis of scaffolds. a) cell morphology on the Gr-CP scaffold for 24 h. b) MTT test on the scaffolds cross linked with 10% and 25% GA for 24 and 72 h.

scaffold that can be measured through tensile experiments. Based on the young's modulus measurements, Gr addition increased the modulus and tensile strength from 46.25 and 3.72 MPa for the CP scaffold to 78.1 and 8.99 MPa for the Gr-CP scaffold, respectively. Similarly, the Gr-CP scaffold exhibited a greater work of fracture (321.60 N.mm) compared to the CP scaffold (225.69 N.mm). Results of the mechanical properties, implying the significant role of Gr in enhancing the mechanical properties of Gr-CP scaffold. The CP scaffold showed a higher elongation (74.62%) compared to the Gr-CP sample (48.84%) (Fig. 3).

### 3.2 Cell morphology and proliferation

Appropriate cell attachment and morphology on a scaffold represent the biocompatibility of scaffold. Attachment of L929 cells to the Gr-CP scaffold 24 h after cell seeding was studied by SEM. Cell morphology and spreading on the scaffold were remarkable only after 24 h (Fig. 4(a)).

MTT analysis was performed to investigate the effect of scaffold extract on cell proliferation. Compared to control samples, L929 cell proliferation levels were 122% and 99% after 24 h and 89% and 82% after 72 h on scaffolds cross linked with 10% and 25% GA, respectively, (Fig. 4(b)). Based on FTIR and MTT results, the scaffold cross linked with 10% GA was selected for subsequent cell differentiation studies.

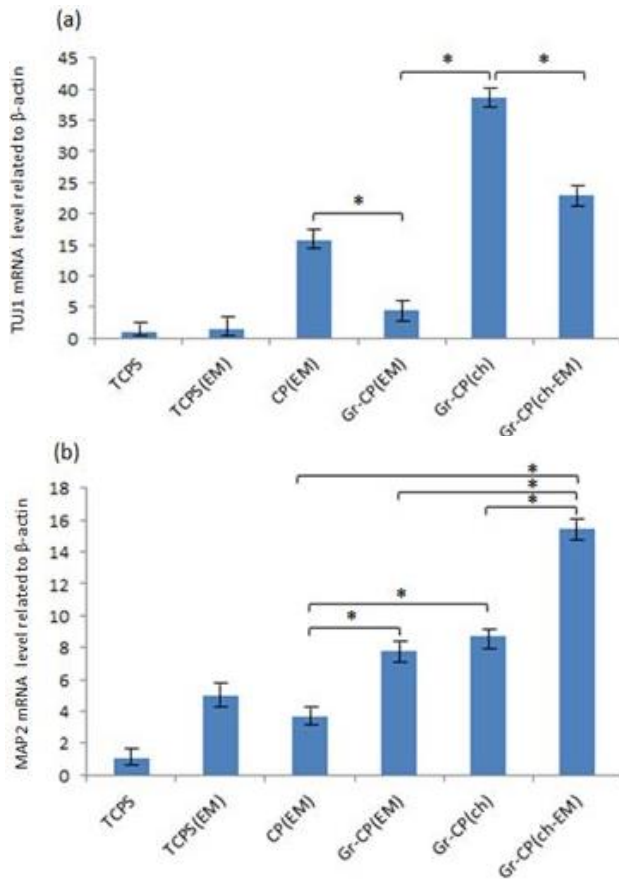


Fig. 5 mRNA expression of differentiation test groups. Real-time PCR results for a) TUJ1 expression and b) MAP2 expression in the TCPS, TCPS(EM), CP(EM), Gr-CP(EM), Gr-CP(ch) and Gr-CP(ch-EM) groups (\*  $P < 0.05$ ).

### 3.3 Neuronal gene expression analysis using real-time PCR

Expression of MAP2 and TUJ1 genes as two neuronal markers was studied through real-time PCR technique. MAP2 is a neuron specific protein which is weakly expressed by neuronal precursors but is significantly expressed by mature neurons (Bojnordi *et al.* 2016, Rapisio *et al.* 2007). TUJ1 is expressed by immature neurons (Bédard and Parent 2004, Callahan *et al.* 2013). The significant expression levels of TUJ1 in the CP(EM), Gr-CP(EM), Gr-CP(ch) and Gr-CP(ch-EM) groups were indicative of neuronal differentiation of RAMSCs. In these groups, TUJ1 expression levels were higher than those of MAP2 (Figs. 5(a) and (b)). As mentioned, TUJ1 is expressed by early neurons and therefore, longer time durations (more than 13 days) were required for differentiation of RAMSCs into mature neurons and observing higher expression levels of MAP2. The observed difference in TUJ1 expression between test groups was indicative of the different effects of signaling factors on neural differentiation. For instance, comparison of TUJ1 mRNA levels in the Gr-CP(ch) and Gr-CP(EM) groups showed that chemical differentiation medium was more neuroinductive than LFEMF.

MAP2 mRNA level was proportional to cell differentiation signals (Fig. 5(b)). Studying cell differentiation mechanisms through LFEMF, Gr and neural chemical medium is essential for analyzing the results of real-time PCR.

Park *et al.* (2013) have reported that EMF can induce NADH, leading to the production of reactive oxygen species (ROS) at the plasma membrane which in turn leads to the phosphorylation of epidermal growth factor receptor (EGFR) and activation of the P13k/Akt intracellular pathway (as a neuronal differentiation pathway).

Gr nanoplatelets have been proved to cause a decrease in mitochondria membrane potential and ROS generation. In fact, one of the drawbacks of Gr is increasing the ROS generation in cells which leads to cytotoxicity and cell death (Ou *et al.* 2016, Zhang *et al.* 2016). Therefore, the appropriate graphene concentration should be determined. In addition to Gr and LFEMF as ROS generating factors, EGF cause neuronal differentiation through increasing cellular ROS and activation of the P13k/Akt pathway (Huo *et al.* 2009, Le Belle *et al.* 2011). So in general, in this study there are three sources of ROS production.

According to the above discussion, the less mature neurons and lower MAP2 expression in the CP(EM) group compared to the Gr-CP(EM) one and also in the Gr-CP(ch) group compared to the Gr-CP(EM-ch) one, had originated from the lower ROS concentrations. This conclusion can be validated based on the Gr-CP(ch-EM) group. ROS is a double-edged sword, as a low ROS concentration is necessary for neuron differentiation and growth while its high concentrations can cause cell apoptosis.

Therefore, due to the increase in ROS concentration by all 3 factors in the Gr-CP(ch-EM) group, cell apoptosis and no expression of MAP2 and TUJ1 genes were expected. Indeed, in our previous study, cell apoptosis was happened due to the simultaneous application of chemical and EM factors that led to an increase in ROS. However, significant expression levels of MAP2 and TUJ1 were observed. The only reason behind such finding may be the presence of BHA in the culture medium of Gr-CP(ch-EM) group. BHA acts as an antioxidant and scavenger of ROS (Festjens *et al.* 2006). In our previous study, no BHA was present in the medium used for the Gr-CP(ch-EM) group, leading to cell death and no expression of MAP2 (Moraveji *et al.* 2016). Comparing the CP(EM), Gr-CP(EM), Gr-CP(ch-EM) groups in our present study and the ch-EM group in our previous work reveals the critical role of ROS in mRNA expression.

## 4. Conclusions

In this present study, a CP fibrous scaffold was prepared through electrospinning and spraying Gr nanoplatelets (1 wt.%) several times through fiber synthesis. Young's modulus, tensile strength and work of fracture of Gr-CP scaffold were increased by 1.68, 2.41 and 1.42 times compared to the CP scaffold, respectively, revealing the positive effect of Gr nanoplatelets on the mechanical properties of scaffolds. In addition, evaluation of L929 cell

adhesion and morphology after 24 h demonstrated excellent cell-scaffold interactions. These results showed that the prepared Gr-CP scaffold can be used as a suitable scaffold for stem cell differentiation. Real-time PCR results were indicative of the positive effects of Gr, LFEMF and chemical medium on neural differentiation. Despite its low cost compared to other differential stimuli, LFEMF was a considerably influential signaling factor. Further studies are still required to investigate cellular pathways and find the optimized conditions for simultaneous application of differentiation factors. In future works, we will study astrocyte and neuron protein expression based on immunocytochemical staining and electrical impedance analysis of scaffold.

### Acknowledgment

This work has been financially supported by Iran National Science Foundation (INSF, grant number: 92027763) and was approved by the Pasteur institute of Iran.

### Conflicts of interest

The authors declare no conflicts of interest. We and our institution at any time don't receive payment or services from a third party.

### References

- Acar, H., Garifullin, R. and Guler, M.O. (2011), "Self-assembled template-directed synthesis of one-dimensional silica and titania nanostructures", *Langmuir*, **27**(3), 1079-1084. <https://doi.org/10.1021/la104518g>.
- Alegret, N., Dominguez-Alfaro, A., González-Domínguez, J.M., Arnaiz, B., Cossío, U., Bosi, S., Vázquez, E., Ramos-Cabrer, P., Mecerreyes, D. and Prato, M. (2018), "Three-Dimensional Conductive Scaffolds as Neural Prostheses Based on Carbon Nanotubes and Polypyrrole", *ACS Appl. Mater. Interf.*, **10**(50), 43904-43914. doi:<https://doi.org/10.1021/acsami.8b16462>.
- Barati, A., Adeli, M.M. and Hadi, A. (2020a), "Static torsion of bi-directional functionally graded microtube based on the couple stress theory under magnetic field", *Int. J. Appl. Mech.*, **12**(02), 2050021. <https://doi.org/10.1142/S1758825120500210>.
- Barati, A., Hadi, A., Nejad, M.Z. and Noroozi, R. (2020b), "On vibration of bi-directional functionally graded nanobeams under magnetic field", *Mech. Based Des. Struct.*, 1-18. <https://doi.org/10.1080/15397734.2020.1719507>.
- Bédard, A. and Parent, A. (2004), "Evidence of newly generated neurons in the human olfactory bulb", *Dev. Brain Res.*, **151**(1), 159-168. <https://doi.org/10.1016/j.devbrainres.2004.03.021>.
- Binhi, V., Alipov, Y.D. and Belyaev, I.Y. (2001), "Effect of static magnetic field on E. coli cells and individual rotations of ion-protein complexes", *Bioelectromagnetics*, **22**(2), 79-86. [https://doi.org/10.1002/1521-186X\(200102\)22:2%3C79::AID-BEM1009%3E3.0.CO;2-7](https://doi.org/10.1002/1521-186X(200102)22:2%3C79::AID-BEM1009%3E3.0.CO;2-7).
- Bojnordi, M.N., Azizi, H., Skutella, T., Movahedin, M., Pourabdolhossein, F., Shojaei, A. and Hamidabadi, H.G. (2016), "Differentiation of Spermatogonia Stem Cells into Functional Mature Neurons Characterized with Differential Gene Expression", *Mole. Neurobiol.*, 1-7. <https://doi.org/10.1007/s12035-016-0097-7>.
- Buchachenko, A.L., Lukzen, N.N. and Pedersen, J.B. (2007), "On the magnetic field and isotope effects in enzymatic phosphorylation", *Chem. Phys. Lett.*, **434**(1-3), 139-143. <https://doi.org/10.1016/j.cplett.2006.12.019>.
- Callahan, L.A.S., Xie, S., Barker, I.A., Zheng, J., Reneker, D.H., Dove, A.P. and Becker, M.L. (2013), "Directed differentiation and neurite extension of mouse embryonic stem cell on aligned poly (lactide) nanofibers functionalized with YIGSR peptide", *Biomaterials*, **34**(36), 9089-9095. <https://doi.org/10.1016/j.biomaterials.2013.08.028>.
- Çapkın, M., Çakmak, S., Kurt, F.Ö., Gümüşderelioğlu, M., Şen, B.H., Türk, B.T. and Delioğlu-Gürhan, S.İ. (2012), "Random/aligned electrospun PCL/PCL-collagen nanofibrous membranes: Comparison of neural differentiation of rat AdMSCs and BMSCs", *Biomed. Mater.*, **7**(4), 045013. <https://doi.org/10.1088/1748-6041/7/4/045013>.
- Cheng, K. and Zou, C. (2006), "Electromagnetic field effect on separation of nucleotide sequences and unwinding of a double helix during DNA replication", *Med. Hypotheses*, **66**(1), 148-153. <https://doi.org/10.1016/j.mehy.2005.07.007>.
- Cho, H., Seo, Y.K., Yoon, H.H., Kim, S.C., Kim, S.M., Song, K.Y. and Park, J.K. (2012), "Neural stimulation on human bone marrow-derived mesenchymal stem cells by extremely low frequency electromagnetic fields", *Biotechnol. Prog.*, **28**(5), 1329-1335. <https://doi.org/10.1002/btpr.1607>.
- Coates, J. (2000), "Interpretation of infrared spectra, a practical approach", In: *Encyclopedia of analytical chemistry: applications, theory and instrumentation*. <https://doi.org/10.1002/9780470027318.a5606>.
- Damink, L.O., Dijkstra, P., Van Luyn, M., Van Wachem, P., Nieuwenhuis, P. and Feijen, J. (1995), "Glutaraldehyde as a crosslinking agent for collagen-based biomaterials", *J. Mater. Sci.-Mater. M.*, **6**(8), 460-472. <https://doi.org/10.1007/BF00123371>.
- Driscoll, N., Richardson, A.G., Maleski, K., Anasori, B., Adewole, O., Lelyukh, P., Escobedo, L., Cullen, D.K., Lucas, T.H., Gogotsi, Y. and Vitale, F. (2018), "Two-dimensional Ti<sub>3</sub>C<sub>2</sub> MXene for high-resolution neural interfaces", *ACS Nano*, **12**(10), 10419-10429. <https://doi.org/10.1021/acsnano.8b06014>.
- Festjens, N., Kalai, M., Smet, J., Meeus, A., Van Coster, R., Saelens, X. and Vandennebeele, P. (2006), "Butylated hydroxyanisole is more than a reactive oxygen species scavenger", *Cell Death Differ.*, **13**(1), 166-169. <https://doi.org/10.1038/sj.cdd.4401746>.
- Gaetani, R., Ledda, M., Barile, L., Chimenti, I., De Carlo, F., Forte, E., Ionta, V., Giuliani, L., D'Emilia, E., Frati, G., Miraldi, F., Pozzi, D., Messina, E., Grimaldi, S., Giacomello, A. and Lisi, A. (2009), "Differentiation of human adult cardiac stem cells exposed to Extremely Low Frequency Electromagnetic Fields", *Cardiovasc. Res.*, **82**(3), 411-420. <https://doi.org/10.1093/cvr/cvp067>.
- Garrudo, F.F., Chapman, C.A., Hoffman, P.R., Udangawa, R.W., Silva, J.C., Mikael, P.E., Rodrigues, C.A.V., Cabral, J.M.S., Morgado, J.M.F., Ferreira, F.C. and Lindhardt, R.J. (2019), "Polyaniline-polycaprolactone blended nanofibers for neural cell culture", *Eur. Polym. J.*, **117**, 28-37. <https://doi.org/10.1016/j.eurpolymj.2019.04.048>.
- Ginestra, P. (2019), "Manufacturing of polycaprolactone-Graphene fibers for nerve tissue engineering", *J. Mech. Behav. Biomed. Mater.*, **100**, 103387. <https://doi.org/10.1016/j.jmbbm.2019.103387>.
- Golafshan, N., Kharaziha, M. and Fathi, M. (2017), "Tough and conductive hybrid graphene-PVA: Alginate fibrous scaffolds for engineering neural construct", *Carbon*, **111**, 752-763. <https://doi.org/10.1016/j.carbon.2016.10.042>.
- Gupta, P., Agrawal, A., Murali, K., Varshney, R., Beniwal, S., Manhas, S., Roy, P. and Lahiri, D. (2019), "Differential neural

- cell adhesion and neurite outgrowth on carbon nanotube and graphene reinforced polymeric scaffolds”, *Mater. Sci. Eng. C*, **97**, 539-551. <https://doi.org/10.1016/j.msec.2018.12.065>.
- He, B., Yuan, X. and Jiang, D. (2014), “Molecular self-assembly guides the fabrication of peptide nanofiber scaffolds for nerve repair”, *RSC Adv.*, **4**(45), 23610-23621. <https://doi.org/10.1039/C4RA01826E>.
- Huo, Y., Qiu, W.-Y., Pan, Q., Yao, Y.-F., Xing, K. and Lou, M.F. (2009), “Reactive oxygen species (ROS) are essential mediators in epidermal growth factor (EGF)-stimulated corneal epithelial cell proliferation, adhesion, migration, and wound healing”, *Exp. Eye Res.*, **89**(6), 876-886. <https://doi.org/10.1016/j.exer.2009.07.012>.
- Jazayeri, M., Shokrgozar, M.A., Haghighipour, N., Bolouri, B., Mirahmadi, F. and Farokhi, M. (2016), “Effects of electromagnetic stimulation on gene expression of mesenchymal stem cells and repair of bone lesions”, *Cell. J. (Yakhteh)*, **19**(1), 34. <https://doi.org/10.22074%2Fcellj.2016.4870>.
- Kavand, H., Haghighipour, N., Zeynali, B., Seyedjafari, E. and Abdemami, B. (2016), “Extremely low frequency electromagnetic field in mesenchymal stem cells gene regulation: chondrogenic markers evaluation”, *Artif. Organs.*, **40**(10), 929-937. <https://doi.org/10.1111/aor.12696>.
- Kenry, L.W., Loh, K.P. and Lim, C.T. (2018), “When stem cells meet graphene: opportunities and challenges in regenerative medicine”, *Biomaterials*, **155**, 236-250. <https://doi.org/10.1016/j.biomaterials.2017.10.004>.
- Khoram, M.M., Hosseini, M., Hadi, A. and Shishehsaz, M. (2020), “Bending analysis of bidirectional FGM Timoshenko nanobeam subjected to mechanical and magnetic forces and resting on Winkler–Pasternak foundation”, *Int. J. Appl. Mech.*, **12**(8), 2050093. <https://doi.org/10.1142/S1758825120500933>.
- Lanza, R., Langer, R. and Vacanti, J.P. (2013), *Principles of Tissue Engineering* (4th Edition ed.), Academic press, Massachusetts, U.S.A.
- Laurence, J.A., French, P.W., Lindner, R.A. and McKenzie, D.R. (2000), “Biological effects of electromagnetic fields—Mechanisms for the effects of pulsed microwave radiation on protein conformation”, *J. Theoretic. Biol.*, **206**(2), 291-298. <https://doi.org/10.1006/jtbi.2000.2123>
- Le Belle, J.E., Orozco, N.M., Paucar, A.A., Saxe, J.P., Mottahedeh, J., Pyle, A.D., Wu, H. and Kornblum, H.I. (2011), “Proliferative neural stem cells have high endogenous ROS levels that regulate self-renewal and neurogenesis in a PI3K/Akt-dependant manner”, *Cell Stem Cell*, **8**(1), 59-71. <https://doi.org/10.1016/j.stem.2010.11.028>.
- Lee, Y.-J., Jang, W., Im, H. and Sung, J.-S. (2015), “Extremely low frequency electromagnetic fields enhance neuronal differentiation of human mesenchymal stem cells on graphene-based substrates”, *Curr. Appl. Phys.*, **15**, S95-S102. <https://doi.org/10.1016/j.cap.2015.04.017>.
- Levin, M. (2009), “Bioelectric mechanisms in regeneration: unique aspects and future perspectives”, In: *Seminars in Cell & Developmental Biology* (Vol. 20, No. 5, pp. 543-556), Academic Press.
- Li, N., Zhang, X., Song, Q., Su, R., Zhang, Q., Kong, T., Liu, L., Jin, G., Tang, M. and Cheng, G. (2011), “The promotion of neurite sprouting and outgrowth of mouse hippocampal cells in culture by graphene substrates”, *Biomaterials*, **32**(35), 9374-9382. <https://doi.org/10.1016/j.biomaterials.2011.08.065>.
- Li, W., Guo, Y., Wang, H., Shi, D., Liang, C., Ye, Z., Qing, F. and Gong, J. (2008), “Electrospun nanofibers immobilized with collagen for neural stem cells culture”, *J. Mater. Sci. Mater. M.*, **19**(2), 847-854. <https://doi.org/10.1007/s10856-007-3087-5>.
- Li, Z., Zhang, Y. and Wang, Y. (2003), “Synthesis and characterization of N-benzoyl-N'-carboxyalkyl substituted thiourea derivatives”, *Phosphorus Sulfur*, **178**(2), 293-297. <https://doi.org/10.1080/10426500307952>.
- Ma, Q., Chen, C., Deng, P., Zhu, G., Lin, M., Zhang, L., Xu, S., He, M., Lu, Y., Duan, W., Pi, H., Cao, Z., Pei, L., Li, M., Liu, C., Zhang, Y., Zhong, M., Zhou, Z. and Yu, Z. (2016), “Extremely low-frequency electromagnetic fields promote in vitro neuronal differentiation and neurite outgrowth of embryonic neural stem cells via up-regulating TRPC1”, *PLoS one*, **11**(3), e0150923. <https://doi.org/10.1371/journal.pone.0150923>.
- Madedec, F., Billaudel, B., de Sauvage, R.C., Sartor, P. and Veyret, B. (2003), “Effects of ELF and static magnetic fields on calcium oscillations in islets of Langerhans”, *Bioelectrochemistry*, **60**(1-2), 73-80. [https://doi.org/10.1016/S1567-5394\(03\)00049-5](https://doi.org/10.1016/S1567-5394(03)00049-5).
- Magaz, A., Spencer, B.F., Hardy, J.G., Li, X., Gough, J.E. and Blaker, J.J. (2020), “Modulation of neuronal cell affinity on PEDOT–PSS nonwoven silk scaffolds for neural tissue engineering”, *ACS Biomater. Sci. Eng.*, **6**(12), 6906-6916. <https://doi.org/10.1021/acsbiomaterials.0c01239>.
- Markov, M. and Pilla, A. (1997), “Weak static magnetic field modulation of myosin phosphorylation in a cell-free preparation: calcium dependence”, *Bioelectrochem. Bioenergetic.*, **43**(2), 233-238. [https://doi.org/10.1016/S0302-4598\(96\)02226-X](https://doi.org/10.1016/S0302-4598(96)02226-X).
- Mohabatpour, F., Karkhaneh, A. and Sharifi, A.M. (2016), “A hydrogel/fiber composite scaffold for chondrocyte encapsulation in cartilage tissue regeneration”, *RSC Adv.*, **6**(86), 83135-83145. <https://doi.org/10.1039/C6RA15592H>.
- Moraveji, M., Haghighipour, N., Keshvari, H., Abbariki, T.N., Shokrgozar, M.A. and Amanzadeh, A. (2016), “Effect of extremely low frequency electromagnetic field on MAP2 and Nestin gene expression of hair follicle dermal papilla cells”, *Int. J. Artificial Organs*, **39**(6), 294-299. <https://doi.org/10.5301/ijao.5000512>.
- Muyonga, J., Cole, C. and Duodu, K. (2004), “Fourier transform infrared (FTIR) spectroscopic study of acid soluble collagen and gelatin from skins and bones of young and adult Nile perch (*Lates niloticus*)”, *Food Chem.*, **86**(3), 325-332. <https://doi.org/10.1016/j.foodchem.2003.09.038>.
- Najafzadeh, M., Adeli, M.M., Zarezadeh, E. and Hadi, A. (2020), “Torsional vibration of the porous nanotube with an arbitrary cross-section based on couple stress theory under magnetic field”, *Mech. Based Des. Struct.*, 1-15. <https://doi.org/10.1080/15397734.2020.1733602>.
- Norizadeh-Abbariki, T., Mashinchian, O., Shokrgozar, M.A., Haghighipour, N., Sen, T. and Mahmoudi, M. (2014), “Superparamagnetic nanoparticles direct differentiation of embryonic stem cells into skeletal muscle cells”, *J. Biomater. Tissue Eng.*, **4**(7), 579-585. <https://doi.org/10.1166/jbt.2014.1205>.
- Ongaro, A., Pellati, A., Bagheri, L., Fortini, C., Setti, S. and De Mattei, M. (2014), “Pulsed electromagnetic fields stimulate osteogenic differentiation in human bone marrow and adipose tissue derived mesenchymal stem cells”, *Bioelectromagnetics*, **35**(6), 426-436. <https://doi.org/10.1002/bem.21862>.
- Ou, L., Song, B., Liang, H., Liu, J., Feng, X., Deng, B., Sun, T. and Shao, L. (2016), “Toxicity of graphene-family nanoparticles: a general review of the origins and mechanisms”, *Particle Fibre Toxicol.*, **13**(1), 57. <https://doi.org/10.1186/s12989-016-0168-y>.
- Ouyang, Y., Huang, C., Zhu, Y., Fan, C. and Ke, Q. (2013), “Fabrication of seamless electrospun collagen/PLGA conduits whose walls comprise highly longitudinally aligned nanofibers for nerve regeneration”, *J. Biomed. Nanotechnol.*, **9**(6), 931-943. <https://doi.org/10.1166/jbn.2013.1605>.
- Özgül, A., Marote, A., Behie, L.A., Salgado, A. and Garipcan, B. (2019), “Extremely low frequency magnetic field induces

- human neuronal differentiation through NMDA receptor activation”, *J. Neural Transm.*, **126**(10), 1281-1290. <https://doi.org/10.1007/s00702-019-02045-5>.
- Park, J.-E., Seo, Y.-K., Yoon, H.-H., Kim, C.-W., Park, J.-K. and Jeon, S. (2013), “Electromagnetic fields induce neural differentiation of human bone marrow derived mesenchymal stem cells via ROS mediated EGFR activation”, *Neurochem. Int.*, **62**(4), 418-424. <https://doi.org/10.1016/j.neuint.2013.02.002>.
- Park, S.Y., Park, J., Sim, S.H., Sung, M.G., Kim, K.S., Hong, B.H. and Hong, S. (2011), “Enhanced differentiation of human neural stem cells into neurons on graphene”, *Adv. Mater.*, **23**(36), <https://doi.org/10.1002/adma.201101503>.
- Pereda, A.E. (2014), “Electrical synapses and their functional interactions with chemical synapses”, *Nat. Rev. Neurosci.*, **15**(4), 250. <https://doi.org/10.1038/nrn3708>.
- Piacentini, R., Ripoli, C., Mezzogori, D., Azzena, G.B. and Grassi, C. (2008), “Extremely low-frequency electromagnetic fields promote in vitro neurogenesis via upregulation of Cav1-channel activity”, *J. Cell. Physiol.*, **215**(1), 129-139. <https://doi.org/10.1002/jcp.21293>.
- Qin, X. and Wu, D. (2012), “Effect of different solvents on poly (caprolactone)(PCL) electrospun nonwoven membranes”, *J. Therm. Anal. Calorim.*, **107**(3), 1007-1013. <https://doi.org/10.1007/s10973-011-1640-4>.
- Rajzer, I., Menaszek, E., Kwiatkowski, R., Planell, J.A. and Castano, O. (2014), “Electrospun gelatin/poly ( $\epsilon$ -caprolactone) fibrous scaffold modified with calcium phosphate for bone tissue engineering”, *Mater. Sci. Eng. C*, **44**, 183-190. <https://doi.org/10.1016/j.msec.2014.08.017>.
- Raposo, E., Guida, C., Baldelli, I., Benvenuto, F., Curto, M., Paleari, L., Filippia, F., Fioccab, R., Robello, G. and Santi, P. (2007), “Characterization and induction of human pre-adipocytes”, *Toxicol. in Vitro*, **21**(2), 330-334. <https://doi.org/10.1016/j.tiv.2006.09.022>.
- Rastin, H., Zhang, B., Bi, J., Hassan, K., Tung, T.T. and Losic, D. (2020), “3D printing of cell-laden electroconductive bioinks for tissue engineering applications”, *J. Mater. Chem. B*, **8**(27), 5862-5876. <https://doi.org/10.1039/D0TB00627K>.
- Rastin, H., Zhang, B., Mazinani, A., Hassan, K., Bi, J., Tung, T.T. and Losic, D. (2020), “3D bioprinting of cell-laden electroconductive MXene nanocomposite bioinks”, *Nanoscale*, **12**(30), 16069-16080. <https://doi.org/10.1039/D0NR02581J>.
- Rohani Rad, E., Vahabi, H., Formela, K., Saeb, M.R. and Thomas, S. (2019), “Injectable poloxamer/graphene oxide hydrogels with well-controlled mechanical and rheological properties”, *Polym. Adv. Technol.*, **30**(9), 2250-2260. <https://doi.org/10.1002/pat.4654>.
- Ryu, S. and Kim, B.-S. (2013), “Culture of neural cells and stem cells on graphene”, *Tissue Eng.*, **10**(2), 39-46. <https://doi.org/10.1007/s13770-013-0384-6>.
- Schnell, E., Klinkhammer, K., Balzer, S., Brook, G., Klee, D., Dalton, P. and Mey, J. (2007), “Guidance of glial cell migration and axonal growth on electrospun nanofibers of poly- $\epsilon$ -caprolactone and a collagen/poly- $\epsilon$ -caprolactone blend”, *Biomaterials*, **28**(19), 3012-3025. <https://doi.org/10.1016/j.biomaterials.2007.03.009>.
- Sionkowska, A., Lewandowska, K. and Adamiak, K. (2020), “The influence of UV light on rheological properties of collagen extracted from silver carp skin”, *Materials*, **13**(19), 4453. <https://doi.org/10.3390/ma13194453>.
- Soleimani, A., Dastani, K., Hadi, A. and Naei, M.H. (2019), “Effect of out-of-plane defects on the postbuckling behavior of graphene sheets based on nonlocal elasticity theory”, *Steel Compos. Struct., Int. J.*, **30**(6), 517-534. <https://doi.org/10.12989/scs.2019.30.6.517>.
- Szymanski, J.M., Jallerat, Q. and Feinberg, A.W. (2014), “ECM protein nanofibers and nanostructures engineered using surface-initiated assembly”, *J. Visual. Experiments: JoVE*, (86), <https://dx.doi.org/10.3791%2F51176>.
- Teo, W.E. and Ramakrishna, S. (2006), “A review on electrospinning design and nanofibre assemblies”, *Nanotechnology*, **17**(14), R89. <https://doi.org/10.1088/0957-4484/17/14/r01>.
- Tonini, R., Baroni, M.D., Masala, E., Micheletti, M., Ferroni, A. and Mazzanti, M. (2001), “Calcium protects differentiating neuroblastoma cells during 50 Hz electromagnetic radiation”, *Biophys. J.*, **81**(5), 2580-2589. [https://doi.org/10.1016/S0006-3495\(01\)75902-4](https://doi.org/10.1016/S0006-3495(01)75902-4).
- Vasita, R. and Katti, D.S. (2006), “Nanofibers and their applications in tissue engineering”, *Int. J. Nanomed.*, **1**(1), 15. <https://dx.doi.org/10.2147%2Fnano.2006.1.1.15>.
- Vijayavenkataraman, S., Thaharah, S., Zhang, S., Lu, W.F. and Fuh, J.Y.H. (2018), “3D-Printed PCL/rGO conductive scaffolds for peripheral nerve injury repair”, *Artif. Organs.*, **43**(5), 515-523. <https://doi.org/10.1111/aor.13360>.
- Wang, Z., Sarje, A., Che, P.-L. and Yarema, K.J. (2009), “Moderate strength (0.23–0.28 T) static magnetic fields (SMF) modulate signaling and differentiation in human embryonic cells”, *BMC Genomics*, **10**(1), 356. <https://doi.org/10.1186/1471-2164-10-356>.
- Wychowanec, J.K., Litowczenko, J., Tadyszak, K., Natu, V., Aparicio, C., Peplińska, B., Barsoumc, M.W., Otyepka, M. and Scheibe, B. (2020), “Unique cellular network formation guided by heterostructures based on reduced graphene oxide-Ti<sub>3</sub>C<sub>2</sub>T<sub>x</sub> MXene hydrogels”, *Acta Biomater.*, **115**, 104-115. <https://doi.org/10.1016/j.actbio.2020.08.010>.
- Xia, Y., Li, S., Nie, C., Zhang, J., Zhou, S., Yang, H., Li, M., Li, W., Cheng, C. and Haag, R. (2019), “A multivalent polyanion-dispersed carbon nanotube toward highly bioactive nanostructured fibrous stem cell scaffolds”, *Appl. Mater. Today*, **16**, 518-528. <https://doi.org/10.1016/j.apmt.2019.07.006>.
- Xie, J., Willerth, S.M., Li, X., Macewan, M.R., Rader, A., Sakiyama-Elbert, S.E. and Xia, Y. (2009), “The differentiation of embryonic stem cells seeded on electrospun nanofibers into neural lineages”, *Biomaterials*, **30**(3), 354-362. <https://doi.org/10.1016%2Fj.biomaterials.2008.09.046>.
- Yin, Y., Huang, P., Han, Z., Wei, G., Zhou, C., Wen, J., Su, B., Wang, X. and Wang, Y. (2014), “Collagen nanofibers facilitated presynaptic maturation in differentiated neurons from spinal-cord-derived neural stem cells through MAPK/ERK1/2-Synapsin I signaling pathway”, *Biomacromolecules*, **15**(7), 2449-2460. <https://doi.org/10.1021/bm500321h>.
- Yoshitani, M., Fukuda, S., Itoi, S.-i., Morino, S., Tao, H., Nakada, A., Inada, Y., Endo, K. and Nakamura, T. (2007), “Experimental repair of phrenic nerve using a polyglycolic acid and collagen tube”, *J. Thorac. Cardio. Sur.*, **133**(3), 726-732. <https://doi.org/10.1016/j.jtcvs.2006.08.089>.
- Zhang, B., Wei, P., Zhou, Z. and Wei, T. (2016), “Interactions of graphene with mammalian cells: Molecular mechanisms and biomedical insights”, *Adv. Drug Deliver. Rev.*, **105**, 145-162. <https://doi.org/10.1016/j.addr.2016.08.009>.
- Zhang, K., Zheng, H., Liang, S. and Gao, C. (2016), “Aligned PLLA nanofibrous scaffolds coated with graphene oxide for promoting neural cell growth”, *Acta Biomaterialia*, **37**, 131-142. <https://doi.org/10.1016/j.actbio.2016.04.008>.
- Zhang, Z., Klausen, L.H., Chen, M. and Dong, M. (2018), “Electroactive scaffolds for neurogenesis and myogenesis: Graphene-based nanomaterials”, *Small*, **14**(48), 1801983. <https://doi.org/10.1002/sml.201801983>.